Liquid-Gated Ambipolar Transport in Ultrathin Films of a Topological Insulator Bi2Te3

ARTICLE *in* NANO LETTERS · JUNE 2011

Impact Factor: 13.59 · DOI: 10.1021/nl201561u · Source: PubMed

7 AUTHORS, INCLUDING:

Hongtao Yuan
Stanford University
66 PUBLICATIONS **1,451** CITATIONS

SEE PROFILE

NANO LETTERS

LETTER

pubs.acs.org/NanoLett

Liquid-Gated Ambipolar Transport in Ultrathin Films of a Topological Insulator Bi_2Te_3

Hongtao Yuan,[*,†,‡] Hongwen Liu,[‡] Hidekazu Shimotani,[†] Hua Guo,[§] Mingwei Chen,[‡] Qikun Xue,[*,§] and Yoshihiro Iwasa[*,†,∥]

[†]Quantum-Phase Electronics Center and Department of Applied Physics, The University of Tokyo, Tokyo, 113-8656, Japan

[‡]WPI Advanced Institute for Materials Research, Tohoku University, Sendai, 980-8577, Japan

[§]Department of Physics, Tsinghua University, Beijing 100084, China

[∥]Correlated Electron Research Group, RIKEN, Wako 351-0198, Japan

Supporting Information

ABSTRACT: Using ionic-liquid (IL) gating in electric-double-layer transistors (EDLTs), we investigate field-effect electrical transport properties of ultrathin epitaxial films of a topological insulator (TI), Bi_2Te_3. Because of their extreme thinness, the Bi_2Te_3 films show a band gap opening and resulting semiconducting transport properties. Near room temperature, an obvious ambipolar transistor operation with an ON-OFF ratio close to 10^3 was observed in the transfer characteristics of liquid-gated EDLTs and further confirmed by a sign change of the Hall coefficients. Modulation of the electronic states and a phase transition from a semiconducting conduction ($dR_{xx}/dT < 0$) to a metallic transport ($dR_{xx}/dT > 0$) were observed in the temperature-dependent resistance of the ultrathin Bi_2Te_3 channel, demonstrating that the liquid gating is an effective way to modulate the electronic states of TIs.

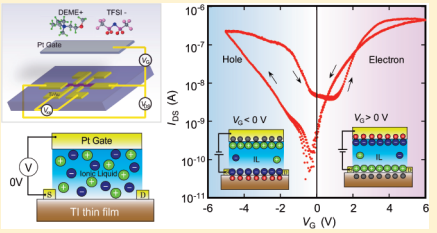

KEYWORDS: Topological insulator, liquid gating, ambipolar transistor, bismuth telluride, electronic transport

As typical Dirac materials with unique band structures where low energy electrons display linear energy-momentum dispersion and can be accurately described by a massless Dirac Hamiltonian, topological insulators (TIs) like Bi_2Te_3 and Bi_2Se_3 are attracting tremendous interest. After their theoretical prediction as three-dimensional TIs[1−3] and experimental confirmation as a new state of quantum matter with an insulating bulk state and metallic Dirac surface states,[4−6] much effort has been devoted to confirm the topological surface states (TSS) from the viewpoint of transport measurements.[7−9] However, electron transport properties of Bi_2Se_3 and Bi_2Te_3 have been always plagued by bulk conduction from the conduction band or intentional and unintentional impurity doping in the bulk samples or cleaved flakes.[10−12] Recently, it has been proved that ultrathin films with intrinsic TI properties can be achieved by using molecule beam epitaxy (MBE) growth, with less influence from the bulk conduction on the transport properties.[13]

Although oxide-gated field-effect transistors have been used as a tool to tune the Fermi level into the "topological" region for observing the surface conduction of TIs,[10−12] there is no definite evidence for ambipolar transport on TI single crystals or flakes by using oxide dielectrics. Electric-double-layer transistors (EDLTs) using ionic liquids (ILs) as gate dielectrics are known to be more efficient in tuning the Fermi energy E_F of solids.[14−20] The electric double layer (EDL) formed at liquid/solid (L/S) interfaces, functioning as nanogap capacitors with a huge capacitance, can effectively accumulate or deplete charge carrier over a large range, resulting in the progresses in electrostatic modulation of interfacial electron states,[18,19] like electric-field-induced superconductivity in $SrTiO_3$ and ZrNCl.[15,16] Therefore, the EDLTs based on such functionalized L/S interfaces might offer a possibility to tune the electronic states and the E_F of solids over a wide range and provide us an opportunity not only to realize the ambipolar transport but also to understand the fundamental physical properties of Dirac materials like graphene[21] and TIs. Another advantage of the EDLTs is their ease for device fabrication processes, where just dropping liquid on film surfaces allows us to make high-performance transistors without complicated and "dirty" lithography processes (TIs are very chemically sensitive to H_2O and organic solvents).

In this Letter, combining the advantages of the high-quality ultrathin Bi_2Te_3 epitaxial films and functionalized EDL interfaces gated by IL dielectrics, we demonstrate an ambipolar operation and the modulation of the electronic states of TI ultrathin films. Bi_2Te_3 films with atomically flat surfaces were grown by molecular beam epitaxy (MBE) in a layer-by-layer mode.[13] A Hall bar configuration with a channel size of 600 μm × 200 μm was patterned by shadow mask patterning processes on a smooth Bi_2Te_3 film. After bonding Au wires on Ti/Au electrodes and installing a Pt plate as the gate electrode, both the channel and the Pt electrode were immersed in a small drop of IL (DEME-TFSI) to form a typical liquid-gated EDL transistor. We stress that the whole process is water-free and the exposure of the TI film to the atmosphere is as short as possible during the device fabrication.

Received: January 9, 2011
Revised: June 19, 2011
Published: June 22, 2011

With the same Hall bar pattern, the transport measurements of Bi_2Te_3 EDLTs, including the transfer characteristics, the longitudinal sheet resistance R_{xx}, and the Hall coefficient R_H, were simultaneously measured in a Physical Property Measurement System (PPMS) combined with a semiconductor parameter analyzer (Agilent 5270B). In order to avoid any possible interfacial electrochemistry between the IL and Bi_2Te_3 channel, transport measurements were mainly performed at 220 K and below, where it has been proved that the interfacial chemistry is significantly suppressed by cooling.[22]

As shown in Figure 1a, atomic layers with a Te−Bi−Te−Bi−Te stacking sequence form a unique quintuple layer (QL) along the

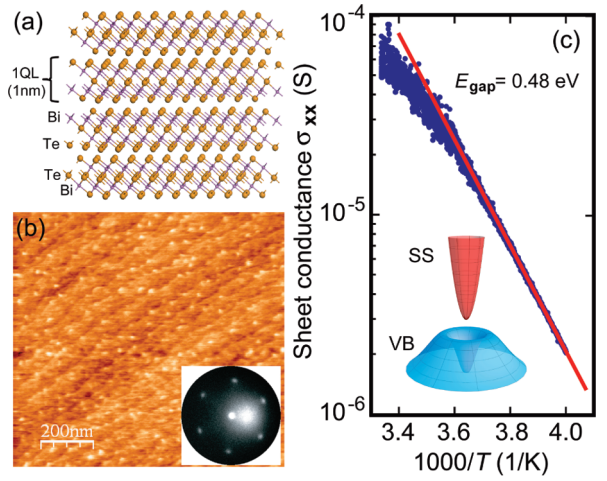

Figure 1. (a) Schematic diagram of the crystal structure of Bi_2Te_3. The weak van der Waals bonding between two adjacent QLs and the strong ionic bonding inside the QLs determine that such a layered system is naturally suitable for realizing a two-dimensional atomically flat surface, which is critical for a transistor channel. (b) An atomic force microscopy (AFM) image and a low energy electron diffraction (LEED) pattern of the as-grown Bi_2Te_3 ultrathin film. (c) Temperature-dependent sheet conductance of the Bi_2Te_3 film with a thickness of 5 nm. The positive temperature coefficient of the conductance ($d\sigma_{xx}/dT > 0$) indicates a semiconducting transport and a band gap opening behavior of the films.

c-axis of the unit cell of rhombohedral Bi_2Te_3. Because of the weak van der Waals bonding between two adjacent QLs, the two-dimensional layered nature is quite suitable for achieving atomically flat surfaces,[23] which are critically important for the transport channel of a field effect transistor. Figure 1b shows an atomic force microscopy (AFM) image and an in situ low-energy electron diffraction (LEED) pattern of the as-grown surface of a Bi_2Te_3 film. The former clearly indicates the step and terrace structures with a monolayer height (1QL, ~3 Å), whereas the latter shows the good crystalline quality of the ultrathin epitaxial film, ensuring the suitability for an EDLT channel. The transport behavior of an as-grown Bi_2Te_3 thin film[13,24] with a thickness of ~5 nm was investigated before dropping IL. As shown in the plot of the sheet-conductance versus inverse temperature ($\sigma_{xx}-1/T$) in Figure 1c, the positive temperature coefficient of the sheet conductance ($d\sigma_{xx}/dT > 0$) clearly suggests the semiconducting transport behavior of the Bi_2Te_3 ultrathin film. Such a behavior was observed in all the ultrathin films we have measured (with thickness of 3−5 nm), implying that the semiconducting transport is reproducible and originates from the intrinsic properties of the ultrathin films. By fitting the $\sigma_{xx}-1/T$ plot with the Arrhenius relationship $\sigma_{xx} = \sigma_0 \exp(-E_a/kT)$, the activation energy E_a of the conductivity (roughly can be regarded as the band gap of the film) was estimated as $E_a = E_{gap} = 0.48$ eV. The value is neither zero, as appropriate for the gapless Dirac cone with surface states nor 0.17 eV between conduction band (CB) and valence band (VB) in bulk crystals, suggesting a band gap opening of the Bi_2Te_3 film (demonstrated in the inset of Figure 1c). Such a large band gap opening between the conduction band and the valence band has been observed in ultrathin TI films with a value around 0.3 eV by using photoemission spectroscopy.[13] The present result confirms the large gap opening in the ultrathin films of Bi_2Te_3 by means of transport experiment. The observed large resistance and semiconducting transport behavior of the Bi_2Te_3 film suggests that the Fermi level E_F of the nonbiased TI ultrathin film is located inside the opened band gap.

Applying the IL as the dielectric for EDLTs (a schematic diagram is shown in Figure 2a,b) allows us to tune the E_F and to realize ambipolar transport in the semiconducting TI ultrathin films. Figure 2c shows the transfer characteristics (source−drain

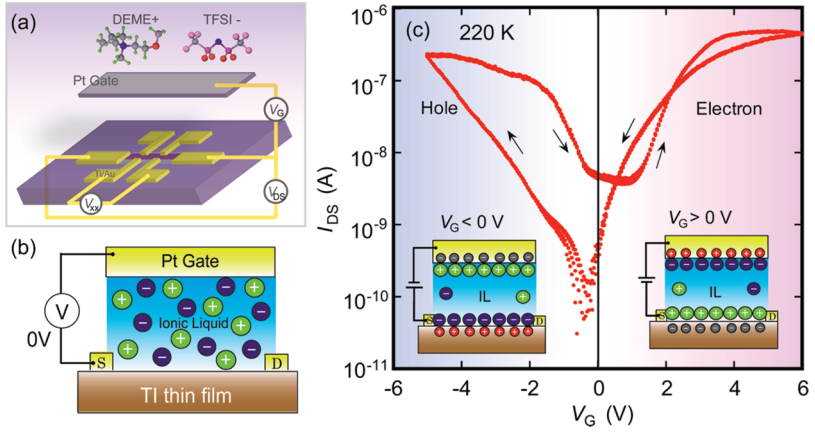

Figure 2. (a) Schematic diagram and (b) cross section of a liquid-gated EDL transistor based on a Bi_2Te_3 film. (c) Transfer characteristics ($I_{DS}-V_G$) of an EDLT based on Bi_2Te_3 ultrathin films at 220 K, showing the ambipolar behavior in transport. Inset: schematic diagram of electron accumulation ($V_G > -0.3$ V) and hole accumulation ($V_G < -0.3$ V) in EDLTs. The transfer characteristics are very reproducible and the curves in three consecutive V_G scans nearly overlap with each other.

dx.doi.org/10.1021/nl201561u |*Nano Lett.* 2011, 11, 2601–2605

current I_{DS} as a function of gate−voltage V_G) of the Bi_2Te_3 EDLT at 220 K. From the schematic inset in Figure 2c, one can clearly see that with the increase of V_G in the positive direction, cations are accumulated right above the film surface and induce the similar amount of electrons in the film, resulting in a dramatic increase of the I_{DS} with electron conduction. On the other hand, when the TI channel is negatively biased, holes are correspondingly accumulated at the interface associated with the increasing I_{DS}. The ON−OFF ratio in the I_{DS} for both hole and electron accumulations is more than 3 orders of magnitude, implying that the electronic states of the channel can be modulated over a wide range. The transfer characteristics in the same devices are very reproducible and the curves of three consecutive scans are almost overlapped with each other. The observed hysteresis may be attributed to the slow ion motion (slow polarization relaxation of liquid dielectric) at 220 K and the interfacial trap states. In order to verify the reproducibility, we made several devices on different batches of ultrathin films. As shown in Figure S1 in Supporting Information, similar ambipolar transfer characteristics have been observed in these Bi_2Te_3 EDLTs.

The V_G dependent sheet resistance R_{xx} in Bi_2Te_3 EDLTs at 220 K, shown in Figure 3b, exhibits a sharp peak with a value more than ten mega-ohms at a low V_G near zero and decays to several kilo-ohms at higher V_G. Such a sharp peak in R_{xx} resembles the field-effect induced ambipolar transport in graphene[21,23] and organic semiconductors.[25,26] The R_{xx} decreases with the increasing bias within a voltage window of $\Delta V_G = \pm 2$ V, which is also similar to the transport behavior of graphene-based transistors[23] and can be qualitatively explained by electron filling into the Bi_2Te_3 band structure. As schematized in Figure 3a, when the gate is negatively biased and holes are accumulated in the Bi_2Te_3 film, the Fermi energy (E_F) is supposed to be tuned to the VB (left diagram in Figure 3a). In contrast, electrons are accumulated when the channel is positively biased, and the E_F is supposed to be shifted to the SS or even up to the conduction band (right diagram). When the bias is near zero, the Fermi level sits inside the opened band gap, resulting in a semiconducting behavior. We note that the charge neutrality point is located at $V_G = -0.3$ V rather than the theoretical value 0 V, implying that the film is electron-doped due to some impurities and interfacial defects.

Figure 3c−e shows Hall effect measurements for various biases at 220 K. One can see from Figure 3c that the Hall coefficient R_H has opposite signs ($R_H < 0$ for electrons and $R_H > 0$ for holes) on different sides from the insulating point ($V_G = -0.3$ V). This behavior directly proves the scenario that the E_F is tuned between VB and TSS (or CB) by the electric field, leading to p-type and n-type conductions, respectively. As shown in Figure 3d, away from the n−p transition point at $V_G = -0.3$ V, the sheet carrier density $n_s = 1/R_H|e|$ (n_s is the sheet carrier concentration and e is the electron charge) in the accumulation layer increases with the bias V_G. Similarly to the increase of the σ_{xx} (decrease in the R_{xx}), the n_s increases linearly with the increasing bias within the ΔV_G window of ±2 V. For a larger V_G, the n_s exhibits a nonmonotonic behavior and starts to saturate by showing a pronounced maximum value. Similar behavior has been observed in EDLTs based on ZnO and organic semiconductors, which was proved to be related to the limitation of the chemical potential window of the IL.[19] The asymmetric behavior for the carrier (e^- or h^+) accumulation might result from two possibilities: one is the asymmetry in the band structures and density of states of VB and TSS (or CB), and the other is the variation in the ion accumulation (cations and anions) at the EDL

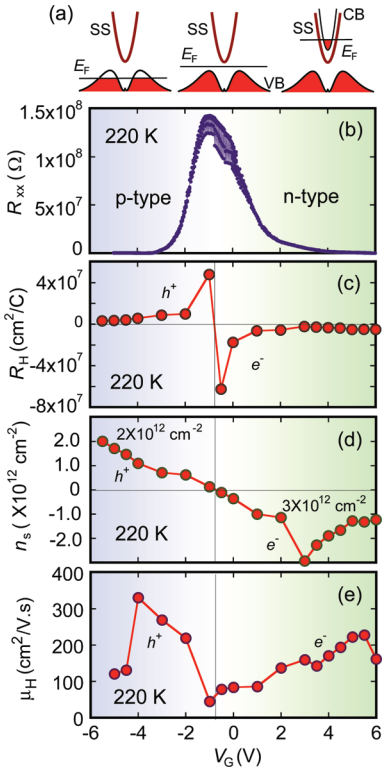

Figure 3. (a) Schematic band structure of the negatively biased (left), zero-biased (middle), and positively biased (right) Bi_2Te_3 film. (b) The sheet resistance R_{xx}, (c) the Hall coefficient R_H, (d) the carrier density n_s, and (e) the Hall mobility μ_H of an EDLT based on an ultrathin Bi_2Te_3 film, as a function of the V_G at 220 K.

interfaces with opposite biases. The estimated Hall mobilities $\mu_H = \sigma_s/|e|n_s$, shown in Figure 3e, with a maximum value around 300 $cm^2/V \cdot s$ for both electrons and holes, was not so high as those reported in the bulk crystals,[27] probably due to interface scattering from defects and lattice mismatch in such an ultrathin film.

In order to confirm that the E_F is really tuned up to the surface states and even to the conduction band from the opened band, we measured the temperature-dependent sheet resistance ($R_{xx}-T$ curve) of the film under a positive bias with electron accumulation. Figure 4 shows the $R_{xx}-T$ curve from 300 down to 200 K. In contrast to the semiconducting behavior in the zero-bias case (blue line, showing wiggles, possibly due to the supercooling of IL), the resistance of positively biased Bi_2Te_3 films (V_G = +2 and +3 V, purple and red lines, respectively) gradually decreases with decreasing temperature. It clearly exhibits a metallic behavior and an absolute conductance larger than the quantum conductance (e^2/h), indicating that the Fermi level is moved up and reaches at least the surface states at the V_G of +2 V. The further decrease in resistance at +3 V might suggest that E_F further moves up to the bottom of the CB band. So far, due to the large contact resistance below 200 K, the transport measurements were mainly carried out above this temperature to ensure reliability.

By simply assuming that all the carriers uniformly exist in the film with a thickness of 5 nm, the 3D carrier density can be deduced as 2×10^{17} cm^{-3} with which the films show an insulating conduction. However, once a large electric field is applied, the carriers are resultingly accumulated in the channel and the thickness of the accumulation layer (the penetration depth of

dx.doi.org/10.1021/nl201561u |Nano Lett. 2011, 11, 2601–2605

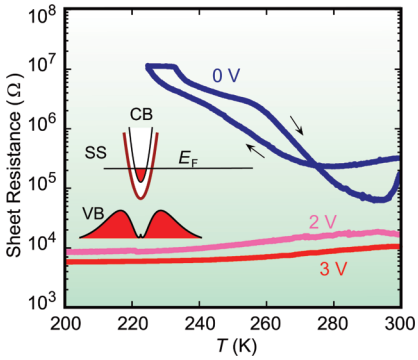

Figure 4. Temperature-dependent resistance of the Bi_2Te_3 EDLT with zero and positive biases. In contrast to the semiconducting behavior in zero-bias case (blue curve), the $R_{xx}-T$ plot of positively biased Bi_2Te_3 films (V_G = +2 V, purple curve) shows a metallic behavior with a conductance larger than the quantum conductance (e^2/h), indicating that the Fermi level has reached the surface states. With increasing the bias to +3 V, further decrease of the R_{xx} might suggest that the Fermi level moved up and touches the bottom of the CB.

applied electric field) decreases. It has been well-known in field effect transistors that the screening length decreases (the thickness of accumulation layer) with increase of carrier density. In the case of another layered material (ZrNCl), the screening length was estimated to be about 1−2 nm.[16] This consideration allows us to roughly assume the charge accumulation layer in the Bi_2Te_3 film as 2 nm. The 3D carrier density under the high electric field can be as large as 1×10^{19} cm^{-3}, deduced by dividing the sheet carrier density $n_s = 2 \times 10^{12}$ cm^{-2} with the estimated thickness (2 nm). Note that only by assuming such a thickness, the 3D carrier density can be reasonably high and sufficient to induce the metallic behavior in the accumulated channel of EDLTs. Further systematic experimental investigations are necessary to clarify the thickness dependent transport and further band filling of the TSS (CB) band as well as resulting low temperature transport in Bi_2Te_3 ultrathin films by means of liquid gating.

In conclusion, with the IL-gated EDLTs, we demonstrated ambipolar transport with a large ON-OFF ratio in ultrathin Bi_2Te_3 films and modulated the electronic properties of the films with electric fields. Ambipolar transistor operation with an ON-OFF ratio close to 10^3 was not only observed in the transfer characteristics of Bi_2Te_3 EDLTs but also confirmed by the sign change of the Hall coefficients in Hall measurements. The EDLTs might be commonly applicable to all types of topological insulator films for effective tuning of E_F in the band structure. Such IL/TI heterostructures involving these intriguing Dirac materials present a new exciting direction in theoretical and experimental researches.

■ ASSOCIATED CONTENT

Supporting Information. Additional information. This material is available free of charge via the Internet at http://pubs.acs.org.

■ AUTHOR INFORMATION

Corresponding Author

*E-mail: (H.Y.) htyuan@ap.t.u-tokyo.ac.jp; (Q.X.) qkxue@mail.tsinghua.edu.cn; (Y.I.) iwasa@ap.t.u-tokyo.ac.jp.

■ ACKNOWLEDGMENT

We wish to thank K. He and A. Tsukazaki for fruitful discussions. This research was partly supported by CREST-JST and Grant-in-Aid for Scientific Research(S) (No. 21224009) from Japan. Y.I. is supported by the Japan Society for the Promotion of Science (JSPS) through its "Funding Program for World-Leading Innovative R&D on Science and Technology (FIRST Program)". Work at Tsinghua University was supported by the National Science Foundation and Ministry of Education of China.

■ REFERENCES

(1) Bernevig, B. A.; Hughes, T. L.; Zhang, S. C. *Science* **2006**, *314*, 1757–1761.
(2) Kane, C. L.; Mele, E. J. *Phys. Rev. Lett.* **2005**, *95*, 146802–4.
(3) Qi, X. L.; Hughes, T. L.; Zhang, S. C. *Phys. Rev. B* **2008**, *78*, 195424–43.
(4) Hsieh, D.; Qian, D.; Wray, L.; Xia, Y.; Hor, Y. S.; Cava, R. J.; Hasan, M. Z. *Nature* **2008**, *452*, 970–974.
(5) Chen, Y. L.; Analytis, J. G.; Chu, J. H.; Liu, Z. K.; Mo, S. K.; Qi, X. L.; Zhang, H. J.; Lu, D. H.; Dai, X.; Fang, Z.; Zhang, S. C.; Fisher, I. R.; Hussain, Z.; Shen, Z.-X. *Science* **2009**, *325*, 178–181.
(6) Xia, Y.; Qian, D.; Hsieh, D.; Wray, L.; Pal, A.; Lin, H.; Bansil, A.; Grauer, D.; Hor, Y. S.; Cava, R. J.; Hasan, M. Z. *Nat. Phys.* **2009**, *5*, 398–402.
(7) Checkelsky, J. G.; Hor, Y. S.; Liu, M.-H.; Qu, D.-X.; Cava, R. J.; Ong, N. P. *Phys. Rev. Lett.* **2009**, *103*, 246601–4.
(8) Analytis, J. G.; Mcdonald, R. D.; Giggs, S. C.; Chu, J. H.; Boebinger, G. S.; Fisher, I. R. *Nat. Phys.* **2010**, *6*, 960–964.
(9) Cheng, P.; Song, C. L.; Zhang, T.; Zhang, Y. Y.; Wang, Y. L.; Jia, J. F.; Wang, J.; Wang, Y. Y.; Zhu, B. F.; Chen, X.; Ma, X. C.; He, K.; Wang, L. L.; Dai, X.; Fang, Z.; Xie, X. C.; Qi, X. L.; Liu, C. X.; Zhang, S. C.; Xue, Q. K. *Phys. Rev. Lett.* **2010**, *105*, 076801–4.
(10) Checkelsky, J. G.; Hor, Y. S.; Cava, R. J.; Ong, N. P. arxiv:1003.3883, 2010.
(11) Chen, J.; Qin, H. J.; Yang, F.; Liu, J.; Guan, T.; Qu, F. M.; Zhang, G. H.; Shi, J. R.; Xie, X. C.; Yang, C. L.; Wu, K. H.; Li, Y. Q.; Lu, L. *Phys. Rev. Lett.* **2010**, *105*, 176602–4.
(12) Steinberg, H.; Gardner, D. R.; Lee, Y. S.; Jarillo-Herrero, P. *Nano Lett.* **2010**, *10*, 5032–5036.
(13) Li, Y. Y.; Wang, G.; Zhu, X. G.; Liu, M. H.; Ye, C.; Chen, X.; Wang, Y. Y.; He, K.; Wang, L. L.; Ma, X. C.; Zhang, H. J.; Dai, X.; Fang, Z.; Xie, X. C.; Liu, Y.; Qi, X. L.; Jia, J. F.; Zhang, S. C.; Xue, Q. K. *Adv. Mater.* **2010**, *22*, 4002–4007.
(14) Cho, J. H.; Lee, J.; Xia, Y.; Kim, B. S.; He, Y.; Renn, M. J.; Lodge, T. P.; Frisbie, C. D. *Nat. Mater.* **2008**, *7*, 900–906.
(15) Ueno, K.; Nakamura, S.; Shimotani, H.; Ohtomo, A.; Kimura, N.; Nojima, T.; Aoki, H.; Iwasa, Y.; Kawasaki, M. *Nat. Mater.* **2008**, *7*, 855–858.
(16) Ye, J. T.; Inoue, S.; Kobayashi, K.; Kasahara, Y.; Yuan, H. T.; Shimotani, H.; Iwasa, Y. *Nat. Mater.* **2010**, *9*, 125–128.
(17) Misra, R.; McCarthy, M.; Hebard, A. F. *Appl. Phys. Lett.* **2007**, *90*, 052905–3.
(18) Ono, S.; Seki, S.; Hirahara, R.; Tominari, Y.; Takeya, J. *Appl. Phys. Lett.* **2008**, *92*, 103313–3.
(19) Yuan, H. T.; Shimotani, H.; Tsukazaki, A.; Ohtomo, A.; Kawasaki, M.; Iwasa, Y. *Adv. Funct. Mater.* **2009**, *19*, 1046–1053.
(20) Dhoot, A. S.; Israel, C.; Moya, X.; Mathur, N. D.; Friend, R. H. *Phys. Rev. Lett.* **2009**, *102*, 136402–4.
(21) Ye, J. T.; Craciun, M. F.; Koshino, M.; Russo, S.; Inoue, S.; Yuan, H. T.; Shimotani, H.; Morpurgo, A. F.; Iwasa, Y. arxiv:1010.4679, 2010.
(22) Yuan, H. T.; Shimotani, H.; Ye, J. T.; Yoon, S. J.; Aliah, H.; Tsukazaki, A.; Kawasaki, M.; Iwasa, Y. *J. Am. Chem. Soc.* **2010**, *132*, 18402–18407.

(23) Novoselov, K. S.; Geim, A. K.; Morozov, S. V.; Jiang, D.; Zhang, Y.; Dubonos, S. V.; Grigorieva, I. V.; Firsov, A. A. *Science* **2004**, *306*, 666–669.
(24) Liu, H. W.; Yuan, H. T.; Fukui, N.; Zhang, L.; Jia, J. F.; Iwasa, Y.; Chen, M. W.; Hashizume, T.; Sakurai, T.; Xue, Q. K. *Cryst. Growth Des.* **2010**, *10*, 4491–4493.
(25) Takahashi, T.; Takenobu, T.; Takeya, J.; Iwasa, Y. *Appl. Phys. Lett.* **2006**, *88*, 033505–3.
(26) Zaumseil, J.; Sirringhaus, H. *Chem. Rev.* **2007**, *107*, 1296–1323.
(27) Qu, D.-X.; Hor, Y. S.; Xiong, J.; Cava, R. J.; Ong, N. P. *Science* **2010**, *329* (5993), 821–824.